Fate of a Sessile Droplet Absorbed into a Porous Surface Experiencing Chemical Degradation

Theresa Atkinson, Homayun K. Navaz, Albert Nowakowski, and Krissy Kamensky
Dept. of Mechanical Engineering, Kettering University, Flint, MI 48504

Ali Zand and Janice Jackson
Dept. of Chemistry and Biochemistry, Kettering University, Flint, MI 48504

DOI 10.1002/aic.14454
Published online April 3, 2014 in Wiley Online Library (wileyonlinelibrary.com)

A general-purpose multiphase and multicomponent computer model was developed for simulation of the spread, evaporation, and chemical reaction of sessile droplet(s) in porous substrates. In the model, chemical reactions were allowed in or between any of the liquid, gas, or solid phases present. The species mass and momentum conservation equations were solved on a finite difference mesh representing the domain. These equations were marched in time using the Runge–Kutta fourth-order method. The model's function was studied via simulation of experiments, both those performed by the authors and found in the literature. These simulations demonstrated a quantitative match to the time history of product evolution and a similar spread of liquid reactants. The model may be particularly beneficial for predicting the extent of contamination and the possible threat outcomes of those chemical agents that are harmful when introduced into the environment. © 2014 American Institute of Chemical Engineers *AIChE J*, 60: 2557–2565, 2014
Keywords: porous media, computational fluid dynamics, reaction kinetics, diffusion (mass transfer, heat transfer)

Introduction

There are numerous engineering applications which involve the spread of a fluid phase within a porous medium. These applications range from oil recovery and other natural formation flows to composites, printing, polymer filling, and fuel cells. The spread of sessile droplets into a porous substrate, which can occur when a liquid is disseminated into the environment, has been addressed in the past.[1–4] However, the spread in the presence of chemical reaction in all phases has not been fully discussed. Specific examples include pesticide spray and deployment of chemical warfare agents. Understanding the interaction of a liquid with a porous material with or without previously existing chemicals inside the pores is critical for determining the fate of toxic chemicals. This problem has environmental, defense, and homeland security implications where assessing the contamination level and the possible need for decontamination is critical to evaluating and mitigating the threat. The studies documented here form an important basis for a modeling approach to detection, protection, decontamination, and remediation following a chemical spill or attack.

Several chemical and physical processes determine the ultimate fate of a droplet, namely: the spread and sorption into a porous substrate, evaporation, and chemical reactions. The coexistence of all these phenomena complicates the prediction of the environmental fate of the droplet.[1–4] For instance, surface evaporation occurs when the surface of a droplet is exposed to surface wind conditions. This problem was previously solved by Navaz et al.[5] and the formulation was incorporated in this model. The model finds the surface evaporation rate of each constituent as a function of temperature, wind speed, and turbulence intensity. Following deposition of a droplet onto a porous surface the fluid absorbs into the media. The absorption rate and spread thread through the media are influenced by the physical environment, for example, the media's porosity and the material properties of the fluid, and chemical processes. Earlier work with this model involved validation of a droplet's spread into the porous media without chemical reaction.[6,7] These studies compared the saturation profile beneath the droplet to experimental data and confirmed the model's ability to provide both qualitative and quantitative results. Briefly, the droplet spread in the model is momentum-driven by the capillary and hydrostatic pressures. The contact area or "foot print" at the base of the drop is defined based on experimental data. There is no spreading of the drop diameter via flow on the free (top) surface, rather the drop's footprint is assumed to be fully saturated with the droplet liquid and fluid flows through to the lower nodes. Overtime, the flow expands further to nodes below and around the droplet. As a fluid penetrates a porous media, evaporation may occur inside the porous medium if any liquid constituent is volatile. This evaporative behavior, termed secondary evaporation, was studied and also previously incorporated into the model.[8] Some liquids may go through a solidification process that will eventually make less liquid phase available to the pores.[9,10] In this work, we have not considered solidification and condensation processes.

Although these earlier studies developed and validated modeling techniques for droplet absorption and evaporation,

Correspondence concerning this article should be addressed to T. Atkinson at tatkinso@kettering.edu.

they did not consider the coupled physiochemical process that may occur. In general, chemical reactions between and within any of the solid, liquid, or gases present in the porous media may occur. Such phenomena can contribute to the fate of droplets.[11–14]

Droplet spread occurs immediately after deposition onto a porous substrate during which a saturation distribution between zero and one exists, necessitating a multiphase flow approach. Therefore, the governing equations need to account for the presence of all phases.[15–17] In these equations, two additional transport parameters are present—relative permeability and a capillary pressure function that includes the interaction parameters between phases.[18] The relative permeability can be modeled using a power function, Brooks and Corey or van Genuchten equations[19,20] where they all have a large number of parameters expressing the relative permeability. The capillary pressure is often modeled using the Leverett *J*-function.[21,22] This capillary pressure function was modified for a sessile droplet by Navaz et al.[23] and it has been used in this work. The environmental fate of a chemical agent is affected by the rates by which all of these processes occur, necessitating a fully coupled approach.

Every chemical in liquid form that is released onto a porous substrate spreads throughout this medium by capillary transport (or pressure), that is, caused by surface tension and viscosity of the liquid. The extent of this capillary transport depends on the physical properties of the liquid (chemical agent) and porous material (substrate). Therefore, the agent/substrate interaction determines the extent of this spread and transport. Additional complication will be encountered when chemical reactions are also present as a part of agent/substrate interaction. One of the most complex problems encountered in the agent/substrate interaction is tracking the chemical of interest as it goes through hydrolysis or other chemical reactions. The moisture and/or water content in the substrate can greatly influence the reaction rate. Chemical species present as reactants or products can be in all phases (solid, liquid, and gas) changing the local physical properties of the substrate. For instance, if the product of a chemical reaction is a solid, the local porosity and permeability of the medium will change, thereby affecting the local capillary pressure. We have taken a continuum approach casting the conservation equations in a domain discretized by finite difference method, allowing the local properties to be different at each node. Zarrouk[24,25] solved one-dimensional transient mass and energy conduction equations with chemical reaction in the solid phase. He also focused on the effect of chemical reaction on the local properties of the porous media such as porosity, permeability, and diffusion. This is mainly due to the creation or depletion of solid phase due to chemical reactions. Numerous earlier works involving chemical reactions in porous media assume a very simple reaction/diffusion model to deal with geological issues[26–28] and solid and ion transport.

To the best of our knowledge, there is no existing general-purpose computer model that couples all existing physiochemical processes by solving fully coupled conservation equations in three-dimensional. The model described here, COMCAD (COmputational Modeling of the Chemical Agent Dispersion), was developed for use in assessing the distribution and temporal behavior of all species, in all phases, undergoing diffusion, evaporation, and chemical reactions. The resulting model can be used to predict the threat of hazardous materials released onto environmental substrates.

Problem Formulation

The continuity and momentum equations for each phase, ignoring the solidification and condensation processes, can be written as:

Conservation of mass for each liquid species

$$\frac{\partial(\varphi\rho_{\ell i}s_{\ell i})}{\partial t}+\nabla\cdot\left(\varphi\rho_{\ell i}s_{\ell i}\overrightarrow{V}_{\ell i}\right)= \left(-\dot{\rho}_{\ell i}^{\text{Secondary}\quad\text{Evaporation}}-\dot{\rho}_{\ell i}^{\text{Surface}\quad\text{Evaporation}}-\dot{\omega}_{\ell i}^{\text{Reaction}}\right) \quad (1)$$

Conservation of mass for each gaseous species

$$\frac{\partial\left(\varphi\rho_{\text{g}j}s_{\text{g}}\right)}{\partial t}+\nabla\cdot\left(\varphi\rho_{\text{g}j}s_{\text{g}}\overrightarrow{V}_{\text{g}j}\right)=\dot{\rho}_{\rho_{\ell i}}^{\text{Secondary}\quad\text{Evaporation}}-\dot{\omega}_{\text{g}j}^{\text{Reaction}} \quad (2)$$

Conservation of mass for each solid species

$$\frac{\partial\rho_{\text{s}k}}{\partial t}=\dot{\omega}_{\text{s}k}^{\text{Reaction}} \quad (3)$$

Momentum equation for liquid species

$$\overrightarrow{V}_{\ell i}=-\frac{Kk_{\ell i}}{\mu_{\ell}}\left(\nabla P_{\ell i}-\rho_{\ell i}gs_{\ell i}\right) \quad (4)$$

Momentum equation for gaseous species

$$\overrightarrow{V}_{\text{g}j}=-\frac{Kk_{\text{g}j}}{\mu_{\text{g}}}\left(\nabla P_{\text{g}j}-\rho_{\text{g}j}gs_{\text{g}}\right)\text{-}D_{j\rightarrow\text{mixture}}\nabla C_{\text{g}j} \quad (5)$$

Where

$$\rho_{\ell}=\sum_{i=1}^{N(\text{Liquids})}\rho_{\ell i}C_{\ell i},\quad C_{\ell i}=\text{Mass}\quad\text{Fraction}=\frac{s_{\ell i}}{s_{\ell}=\sum_{i=1}^{N}s_{\ell i}},\quad \mu_{\ell}=\sum_{i=1}^{N(\text{Liquids})}\mu_{\ell i}C_{\ell i},\quad P_{\ell i}=P-P_{ci}$$
$$s_{\text{g}}=1-\sum_{i}^{N(\text{Liquids})}s_{\ell i},\quad \rho_{\text{g}}=\sum_{j=1}^{M(\text{Gases})}\rho_{\text{g}j}C_{\text{g}j},\quad C_{\text{g}j}=\text{Mass}\quad\text{Fraction}=\frac{\rho_{\text{g}j}}{\rho_{\text{g}}},\quad \mu_{\text{g}}=\sum_{j=1}^{M(\text{Gases})}\mu_{\text{g}j}C_{\text{g}j} \quad (6)$$

$\mu_{\ell i}$, $\rho_{\ell i}$, $s_{\ell i}$, $P_{\ell i}=P-P_{\text{c}i}$ are, respectively, the viscosity, density, saturation, and pressure of liquid phase constituent "*i*." $P_{\text{c}i}$ is the capillary pressure for liquid "*i*." *g* is the gravitational acceleration in the desired direction. $\mu_{\text{g}j}$ and $\rho_{\text{g}j}$, are the viscosity and density of each constituent in the gas phase. $\dot{\omega}$ is the rate of chemical species production/destruction in the related phase, *k* is the relative permeability, and $\phi=\phi(\rho_{\text{s}k})$ is the local porosity, and $D_{j\rightarrow\text{mixture}}(\varphi,s_{\ell})$ is the

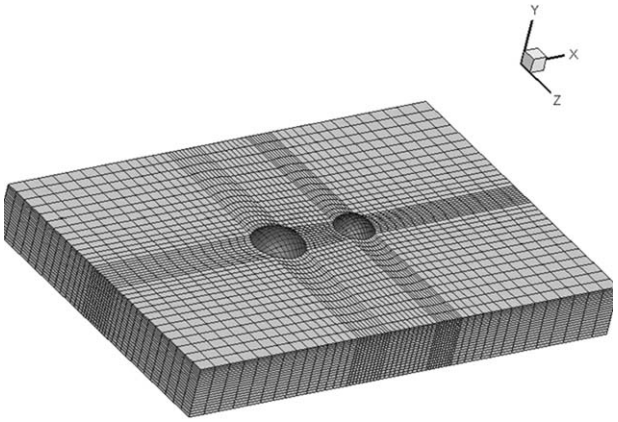

Figure 1. A typical mesh for two droplets (VX and water) generated by COMCAD code.

Each bound may be set to simulate evaporating, impermeable, or infinite conditions. Single drops are automatically generated in the center of the top surface using the experimentally obtained droplet radius or contact angle and droplet volume.

effective diffusion coefficient defined as molecular diffusivity of each gas constituent into the mixture attenuated by the local porosity and saturation. K is the saturation permeability.

The molecular diffusion coefficient, as a function of temperature, is obtained based on the methodology in Treyball.[29] The molecular diffusivity is modified using a function obtained from experimental data[8] based on local porosity and saturation

$$D_i(T,\varphi,s_\ell)=\Big[-0.5855(1-s_\ell)^3+0.4591(1-s_\ell)^2 +0.1264(1-s_\ell)\Big]\varphi(x,y,z,t)D_{j-\mathrm{Mix}}(T)$$

with

$$s_\ell=\sum_{i=1}^{N}s_{\ell i}$$

The relative permeability is taken to be $k_{r\ell i}=s_{\ell i}^2$ based on experimental and modeling studies.

All analysis is carried out under isothermal conditions.

The COMCAD computer model solves the species mass and momentum conservation equations on a finite difference mesh in transformed coordinates, and not physical coordinates. The detailed numerical technique is explained in our earlier work[5–8,23,30] and will not be repeated here. The COMCAD code has an internal grid generation module that can automatically generate a mesh for two droplets at any proximity. The mesh can be stretched in any direction by the user defined parameters, where steep gradients are expected. Figure 1 shows a typical mesh for two droplets.

The droplets are constructed in the form of a spherical cap. However, general shaped droplets and mesh can be constructed externally by ^{TM}GRIDGEN[31] program and imported into the COMCAD code. It should also be mentioned that the droplet spread prediction by the model is very accurate and the results are presented in our earlier works[5,8,23,30] and will not be repeated here. We will instead present the model performance in the presence of chemical reactions.

Chemistry Model

In general, a chemical reaction is modeled using the relationship

$$\sum_{i=1}^{N}v_i'M_i\rightarrow\sum_{i=1}^{N}v_i''M_i \tag{7}$$

Where N, v_i', v_i'', M_i are the number of chemical species present, stoichiometric coefficient for species as reactant, stoichiometric coefficient for species as product, and the mole fraction of each species, respectively. For species not involved in a reaction v_i is zero. Multiple reactions are considered to occur together at any instant in time, with the source/sink term formed as the summation of the effects of all reactions in each species at each node. The specific chemical reaction rate (k_{Rate}) is, in general, a function of temperature. The model utilizes the Arrhenius law to describe this dependence

$$k_{\mathrm{Rate}}=A\exp\left(\frac{-E_{\mathrm{a}}}{RT}\right) \tag{8}$$

Where A, E_{a}, R, and T are the pre-exponential factor, accounting for collision terms and the steric factor associated with the orientation of the colliding molecules, the activation energy, the universal gas constant, and temperature, respectively. For those cases where the activation energy is unknown, but the rate of the reaction at the temperature of interest is known, E_{a} is set equal to zero resulting in a constant reaction rate. As this model does not include the energy equation, all analysis is carried out at constant temperature, therefore, k_{Rate} remains constant during the simulation.

The net rate of production/destruction of species (in nondimensional form) is

$$=\left(v_i''-v_i'\right)k_{\mathrm{Rate}}\left(C_M\right)^m\prod_{j=1}^{N}\left(X_j\right)^{r_j} \tag{9}$$

Where $m=\sum_{j=1}^{N}r_j$ is the order of the reaction, which is based on the user specified reaction rate coefficients for each species, X_j is the mole fraction of species j at each point, and C_M is the total concentration of species. For example, in a reaction characterized using a first-order reaction rate function, r_j would equal 1 for the rate determining species and zero for all others. The reaction rates and the form of the rate equation are based on experimental data. Reaction rates may be obtained from observed reaction kinetics in the environment of interest (i.e., liquids applied to sand) or obtained via homogeneous (aqueous) reactions for the conditions of interest (i.e., constant pH, constant temperature).

Where experimental data results in rate equations that are taken as pseudo-order based on excess of a reactant in an experiment, the same form may be applied within the model. However, as the model applies the reaction locally, it is possible that the assumption of excess reactant may be violated at some points. To deal with this issue, the code first identifies pseudo-order reactions, then monitors the levels of all reactants at each location. If the available moles of a reactant which was not included in the reaction function fall below those of the included reactant(s), the reactant with the lowest availability is used instead. This results in a reduced rate or potentially ceased reaction for that point.

For liquid–liquid reactions and liquid–solid reactions, where the reaction kinetics are based on homogeneous reaction data, the conditions in the porous media may deviate

Table 1. Simultaneous Reactions for VX in Sand Simulation

Reaction	Rate Constant [1/s]	Reaction Model
C10H19O6PS2 + OH− − C8H15O6PS2 + C2H6O	1.6 e-6	K[Mal]
C6H12O + H3PO4 − C6H10 + H3PO4 + H2O	1.93e-4	K[C6H11OH]
VX − EMPA + DESH	8.3e-6	K1[VX]
VX − VXH+	2.3e-5	K2[VX]
VXH+ − EMPA+DESH	1.06e-5	K3[VXH+]
VX − EMPT + DIAZ+	1.71e-6	K4[VX]
VX – EA-2192 + EtOH	2.75e-6	K5[VX]
Na2S(s) + H2SO4 − Na2SO4 + H2S(g)	5.02e-4	K[H2SO4]

EMPA($CH_3P(O)(OC_2H_5)OH$); DESH($HSCH_2CH_2N(isoPr)_2$); EA-2192($CH_3P(O)(OH)SCH_2CH_2N(isoPr)_2$); EMPT($CH_3P(O)(OC_2H_5)SH$)

from ideal when reactant concentrations are very low. For these conditions, the mixed assumption may be violated. To handle this in the model, the reaction rate is decreased by an order of magnitude when the reactant concentration at a node falls below 1%. In this way, the model modifies the reaction kinetics to reflect a crossover to a diffusion controlled system, without including detailed micromechanics. As the code is intended for use in monitoring total chemical present in a macroscopic system, this approach provided a reasonable reflection of the local environmental effects. The code allows the user to vary the concentration limit where this crossover occurs and the magnitude of the rate change, or to eliminate it completely. The modularity of the COMCAD code allows for future inclusion of a more detailed representation of local mixing effects, if these were to be required for a specific application.

In the model species, mole fractions are calculated based on phases active in the reaction, which may involve liquid, solid, and gas phases. For instance, if the reaction only involves liquids, the mole fractions will be calculated using the total moles for all liquids present at a point. The mole fraction therefore provides a relative concentration measure for species involved in a reaction.

Where a reaction involves a solid, local solid volume is recalculated at each time step based on the solid mixture density. This information is used to update the local porosity and permeability.

These mixture and production/destruction calculations are carried out point wise in the porous media, thereby providing a local measure. Total quantities of chemical species are obtained through integration across the domain at each time. The time-step size in a simulation may be varied to optimize solution time and accuracy. Multiple trials were performed to determine appropriate time-step size. Steps on the order of 0.1 ms were adequate to capture processes occurring during imbibition of the droplet(s), while larger time steps ranging up to 1.0 s were applied once the simulated process were dominated by slow reactions or diffusion with rates on the order of 10^{-4} s.

Results and Discussion

Numerous test cases were selected to validate the model, exemplar cases are included here. All of the test cases were performed isothermally. Therefore, any influence of temperature variation on reaction rates or chemical properties was eliminated. In each experiment, the same sand was used, with a measured porosity of 35%. The saturation permeability in the model is a function of porosity based on experimental data,[6–8] which yielded $6.9e^{-12}$ m^2.

Hydrolysis: Malathion reaction with water inside soil

Reaction of chemical agents or pesticides with water is of special interest because it describes a common degradation pathway. It, therefore, presents a practical application due to the natural existence of moisture inside soil or environmental substrates. Malathion, an organophosphate widely used in agriculture as a pesticide, has physical properties similar to the nerve agent VX, especially their multiple reaction centers. Malathion degrades very slowly at low pH, but can undergo rapid hydrolysis in basic solutions.[32] To minimize the time scale required for the bench experiments, conditions of high pH and temperature were utilized. Similar conditions occur on hydrated concrete and in some natural waters.[32] In these experiments, Malathion was mixed into wetted sand. The porosity of commercially available play sand was measured to be 35%. The sand was prepared with a buffer (potassium carbonate solution) to maintain a pH of 10. A solution of 6.15 g of Malathion suspended in 100-mL acetone was prepared and a 2-mL aliquot (total applied dose: 0.125 g/3.72 $\times$ 10^{-4} moles) of Malathion was spread on 25 g of sand. This was then mixed to achieve a consistent concentration of reactant when the acetone evaporates. Preliminary studies demonstrated negligible degradation of the Malathion during the drying process. Distilled water was added to the dried sand and achieves a 35% saturation level. A set of 15 sample jars were filled with the sand. The containers were capped and sealed then maintained at 50°C. At regular intervals, a jar would be selected for analysis and the amount of Malathion remaining quantified using a gas chromatogram (GC).

The sand mixture was simulated using the experimental vial dimensions for the porous media in the model. A uniform concentration of Malathion was applied, such that the total mass of Malathion in the model matched that used in the experiments. The model assumed uniform mixing and porosity and no evaporation. The hydrolysis reaction was assumed to be pseudo-first-order in Malathion, based on the experimental conditions and observed Malathion degradation. The reaction rate constant was based on liquid 1.6e-6 s^{-1} (Table 1), and was similar to that reported in basic environments.[32] The results were compared to those for Malathion in the sand solution (Figure 2). The similarity between the time history of Malathion present in the model and that measured in the

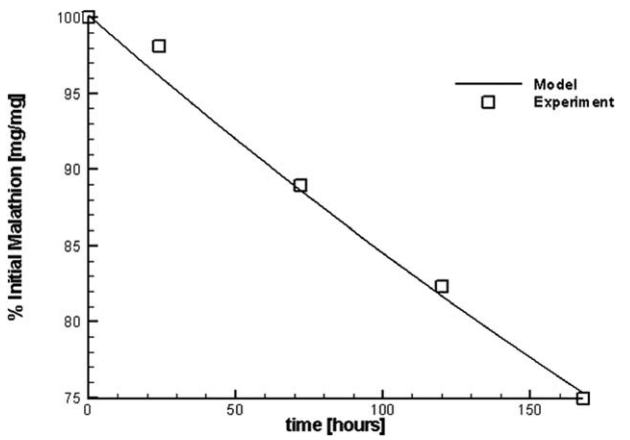

Figure 2. Malathion destruction through hydrolysis in sand at pH of 10 and 50°C.

The squares indicate average measures from the experimental study.

experiment suggest that the uniform concentration assumption and first-order reaction formulation applied here were adequate to capture the overall physics of the sand environment.

In this experiment, the degradation of Malathion was somewhat independent of the local environment, likely due to the excess of basic water present and the constant temperature control. In this case, it is likely that there are sufficient hydroxyl ions to maintain an approximately constant degradation. In a natural setting, where the local environment might vary, a higher order reaction function which includes the hydroxyl concentration might be required to provide an adequate representation. Although this model is capable of performing this simulation, this was not studied here.

Liquid/liquid reaction—Cyclohexanol and phosphoric acid

To further examine the model's capability to reflect reactions between liquids occurring in porous media, it was applied to model an experiment where two liquids diffuse together and react. This experiment was intended to verify the model's coupled formulation for diffusion and reaction. It also represents a rain event where water and the chemical of interest are applied simultaneously. Here, the chemicals involved were selected to provide a faster reaction rate and evaporation, which were also intended to challenge the model formulation. In this set of experiments, the porous media consisted of Petri dishes filled with 25 g of glass beads. Into these beads, equimolar droplets of cyclohexanol and phosphoric acid (cyclohexanol 89.5 μL, phosphoric acid 50 μL) were placed 99.5 mm apart leaving 1 mm between edges of the drops (as defined by earlier trials). The depth of glass beads was 0.6 cm and the porosity was 0.35. The reaction produced cyclohexene when the two droplets came into contact following capillary diffusion.

At each time point 5, 15, 30, and 45 min, the amount of cyclohexanol remaining was quantified using a GC. Experiments at each time point were performed in triplicate. The droplet radius was measured on photographs of each experiment (ImageJ, NIH) and the average used in creating the model geometry. A second set of experiments, where cyclohexanol alone was applied to Petri dishes (eliminating the reactive loss) was performed to identify evaporative losses. The evaporative loss of cyclohexanol was deducted from the experimental data to arrive at an estimate of the loss due to reaction alone, and this data was used to provide the reaction rate for the model (Table 1). The reaction was taken as pseudo-first-order based on the experimental data. The model was created to represent the physical dimensions of the experiment, with the model's side edges extending beyond the field of droplet spread and an infinite boundary condition imposed. The model's depth was equal to the depth of glass beads and the bottom boundary set as impermeable to simulate the petri dish.

The simulation produced a droplet spread which was similar to that seen in the experiments. In Figures 3a, b, where total saturation (V_{liquid}/V_{void}) at 30 s is plotted, the extent of spread is visualized. The plot also indicates lower saturation in the cyclohexanol droplet footprint relative to that for phosphoric acid. This highlights the role of viscosity in the droplet spread, as the lower viscosity of the cyclohexanol allows for faster flow in the porous media, therefore, more spread and lower saturation. Figure 3c shows the saturation field at later time, when a region of mixing has developed between the droplets. The mixing region between the droplets grows as they spread. Initially droplet spread is governed by gravity and capillary pressure, as described in the momentum equation. These initial processes occur relatively rapidly. Numerical studies prior to running a complete simulation were made to select an appropriate time-step size. In

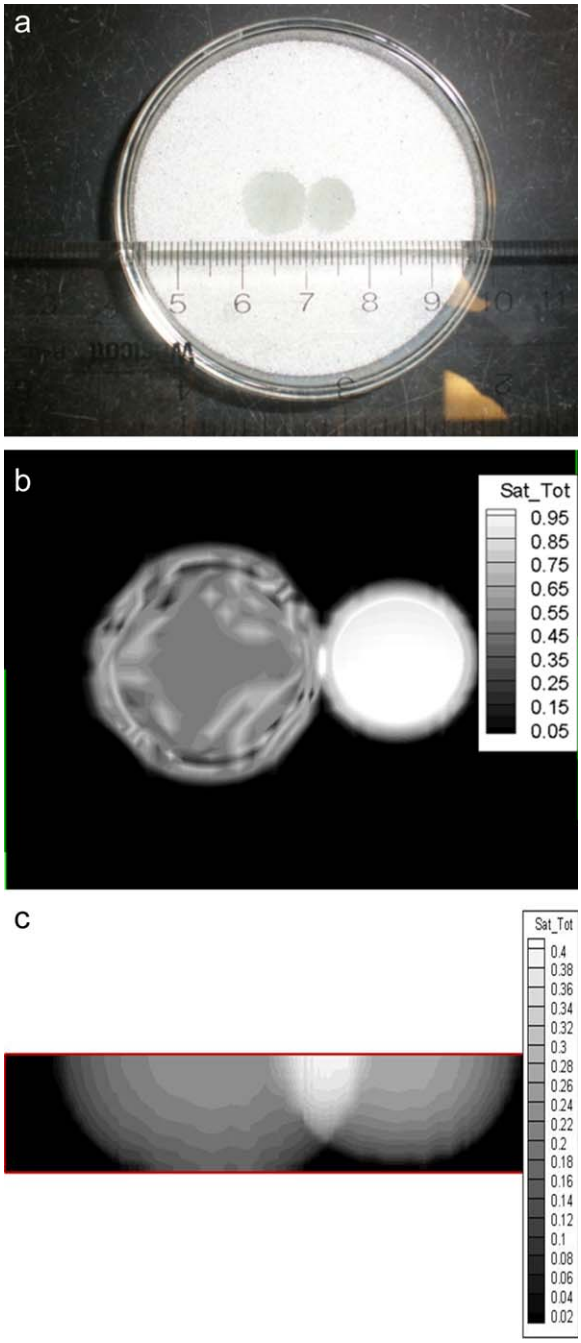

Figure 3. Cyclohexanol/phosphoric acid diffusion and reaction.

Image [a] illustrates a typical experiment approximately 30 s after deposition of the droplets. Image [b] shows the model at the same time point. In both image [b] and [c] the local liquid concentration is shown as total saturation (Sat_Tot = V_{liquid}/V_{void}). Image [c] shows fluid spread and mixing at 60 min, where the light area in the center is the region of highest saturation (mixed reactants) and highest production of cyclohexene. [Color figure can be viewed in the online issue, which is available at wileyonlinelibrary.com.]

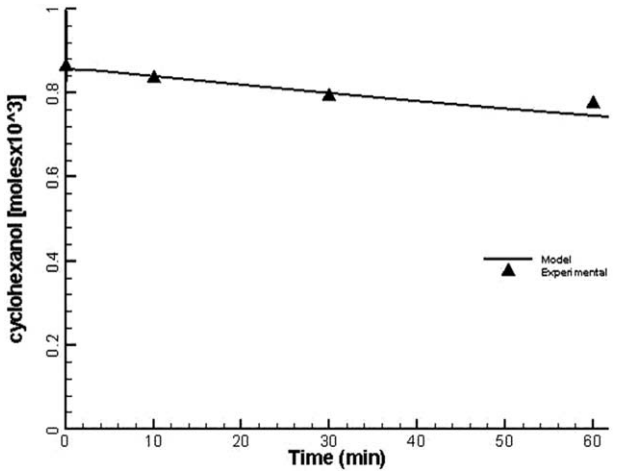

Figure 4. Cyclohexanol disappearance in liquid–liquid reaction.

this case, 0.1 ms for the first 5 s. The later growth of the mixed region (after 10 s), is governed by liquid movement driven primarily by capillary pressure.[33] As the droplet spreads, the saturation at the peripheral pores decreases and the liquid velocity slows. The capillary pressure driving force continues to decrease until, after several minutes, the droplet spread has essentially ceased. During this portion of the simulation the time step varied from 1 ms up to a maximum of 0.5 s after 30 min simulated time.

Cyclohexanol disappearance in the model is function of the local concentration of each reactant. The amount of each reactant present at a point drives the rate of evolution of cyclohexene and therefore the amount present varies across the mixed region. As the amount of cyclohexene, a lower viscosity liquid, increases in the mixed interface region one might expect this region to spread. This is not the case in the model, as the momentum function utilizes the mixture viscosity, which is dominated by the much more viscous phosphoric acid. This behavior visually appears to capture the spread behavior observed in the experiments, however, the data gathered in the experimental study did not allow for precise measurement of the spread.

The time scale of the spread in the model is on the order of a minute, while the half-life of cyclohexanol is on the order of hours. The difference highlights the relative roles of capillary flow and diffusion. The capillary flow is required to create a mixed region, but once it is created the reaction proceeds slowly. Although earlier work validated the fluid spread simulation capability in the model,[6–8,33] this experiment further suggests that the mixing and diffusion algorithms are reasonable, given the concentration field it produced here yielded a total production of cyclohexene at each time point similar to that in the experiments (Figure 4).

In this simulation, the model's mass weighted mixing of properties appears to have provided physically realistic flow and mixing. However, the experiments did not involve measurement of local concentrations of reactants and products. Such measures would provide further confidence in the model's formulation and should be the focus of future work. Some highly viscous liquids may not be well described by the mass weighted mixture model.[34] In these cases, an experimentally based mixture rule may be required. This model's formulation is sufficiently flexible to allow inclusion of such formulations as needed for a particular case.

Liquid/liquid reaction—VX and water (pre-existing-moist sand)

To examine the model's response to multiple chemical reaction processes that are influenced by the spread of a droplet, a simulation of a 6-μL droplet of O-ethyl s-[2-N,N-(diisopropylamino)ethyl]methylphosphonothioate (VX) was created. The droplet was allowed to spread into a media with porosity of 35%. The rates of hydrolysis reaction were defined based on those reported in Brevett et al.[12] for VX reacting on moist sand. Briefly, VX degrades into several breakdown products (Table 1) in wet sand. The droplet base radius was also taken from this study.

All of the degradation reactions were approximated as first-order in VX, due to the large excess of water (experiments reported a 25–32 fold molar excess). The model sides and base extended beyond the field of droplet spread and were set as impermeable. The degradation took place under sealed conditions and was, therefore, modeled without evaporation. The model indicated VX disappearance and appearance of breakdown products in quantities similar to those reported in the experimental study (Figure 5). Fluid spread to a radius of 7 mm was similar to that reported in experiments by Brevett et al.[12] The quantitative match between the experiment and model during the appearance and subsequent destruction of VXH+ demonstrates the model's ability to handle multiple reactions though sequential application of each reaction at each time step and node. The local rate of production/destruction of each chemical species varies across the saturation profile within the sand, yielding a complex mixture of species. If the model's fluid motion were inappropriate the local concentrations would cause the local rates of production/destruction (based on local concentrations in the reaction model) to be inappropriate. The match to experimental data therefore lends support to both the fluid motion and reaction modeling methods.

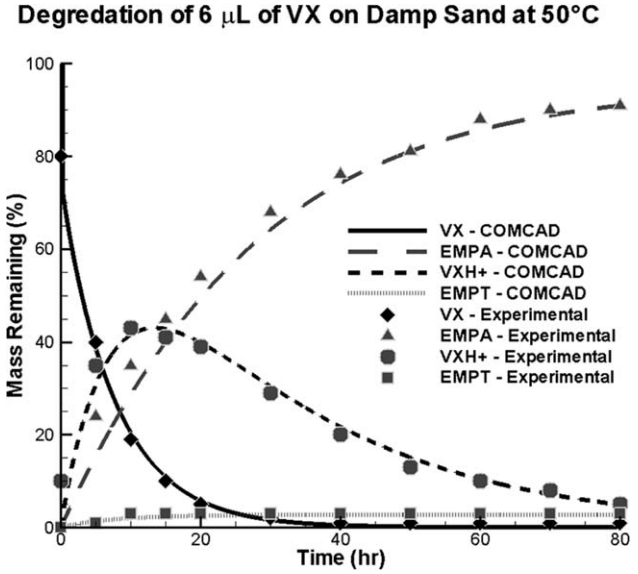

Figure 5. A 6-μL VX droplet undergoes hydrolysis in damp sand at 50°C.

Both agent and breakdown product amounts present in the sand, as measured in Brevett et al.'s [12] experimental study, are characterized by the model.

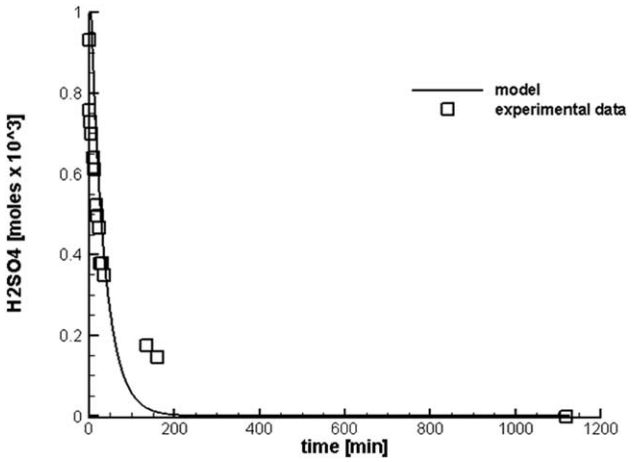

Figure 6. Model predicted loss of liquid sulfuric acid in a reaction between a solid sodium sulfide brick and 50-μl liquid droplet of sulfuric acid.

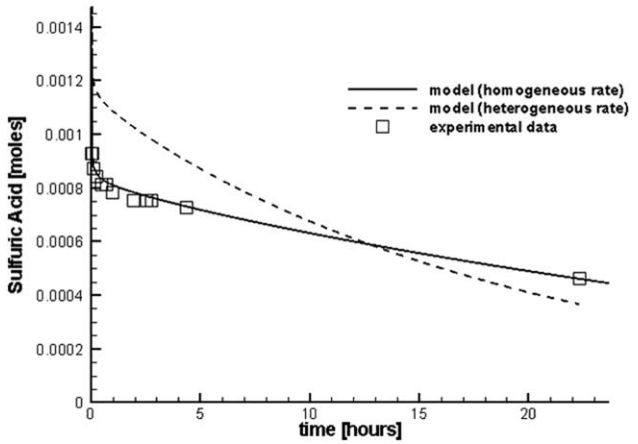

Figure 7. Model and experiment comparison for a porous media mixture of 75% sand and 25% sodium sulfate and a 50-μL droplet of sulfuric acid.

The reaction rate derived from the so called "homogeneous" experiment (100% sodium sulfide) and the rate lowering algorithm (for low reactant availability) gives a better match to the experimental data.

Solid/liquid reaction

In this experiment, a 50-μL droplet of sulfuric acid (liquid phase) reacts with a brick of sodium sulfide (solid phase, approximately 20 × 20 × 15 mm^3). The chemical reaction takes place according to:

$$Na_2S_{(s)} + H_2SO_{4\,(aq)} \rightarrow Na_2SO_{4\,(s)} + H_2S_{(g)}$$

This experiment was selected to verify the model's ability to handle reactions between different phases. The ability to handle reactions between solids and liquids is of key interest in the study of solid remediation agents, which can be mixed into soils. Therefore, the ability to model these situations was deemed important.

The experimental study involved tracking the mixture mass over time to find the amount of hydrogen sulfide evolved. The rate of loss for sulfuric acid was calculated based on this measure. The resulting rate (pseudo-first-order in sulfuric acid) was applied in the COMCAD model. The results are shown in Figure 6, where a quantitative as well as a qualitative match to the experimental data is demonstrated.

Although this simulation provided verification of the communication between the phases involved in the reaction, it also provided an excess of both reactants. This situation did not represent the mixed solid environment present in many soils or sand/decontaminant mixes. To study the model's ability to capture reactions in mixed solid media, a second experiment was performed. Here, a 50-μL droplet of sulfuric acid was placed on a media that consisted of a mixture of 25% sand and 75% sodium sulfide. The droplet radius was measured on photographs made during the experiment (ImageJ, NIH). The rate of reaction was obtained based on mass loss. In the model, this experiment was simulated in two ways: using a reaction rate based on the sulfuric acid half-life observed from this sand/sodium sulfide experiment and using the reaction rate obtained from the 100% sodium sulfide experiment. The 100% sodium sulfide case approximated homogeneous conditions for this reaction. When the rate of destruction of sulfuric acid in the simulations were compared to the experimental data, the simulation using the homogeneous reaction rate, where low reactant concentration triggers a reduced reaction rate in the model, provided a superior characterization of the experimental data (Figure 7). The fit to the initial portion of the degradation curve suggests that the local environment can be well characterized using the reaction rate from the homogenous (liquid on solid sodium sulfide) case. This is consistent with a physical environment where pores are filled with fluid and well mixed conditions exist. The ability of the model to characterize the longer term data suggests that the model algorithm to handle low reactant concentrations is reasonable. After the initially fast reaction, the model transitions to a slower reaction rate, characteristic of a reaction where diffusion mechanisms dominate. This transition occurs at different nodes in the wetted area, but the overall effect is smooth. In both simulations, the extent of spread of the liquid in the model was similar to the diameter of the "clump" found in the sand after the reaction (~15 mm). Figures 8 and 9 describe the location and flow of fluid and gas, respectively, in the simulated porous environment. When solution images are animated, one observes a flow field where gas evolving in the acid saturation zone flows toward the edges and out through the upper surface of the model. This flow pattern illustrates the forces driving gas motion in the simulated environment. Partial pressure driven flow moves H_2S gas from regions of

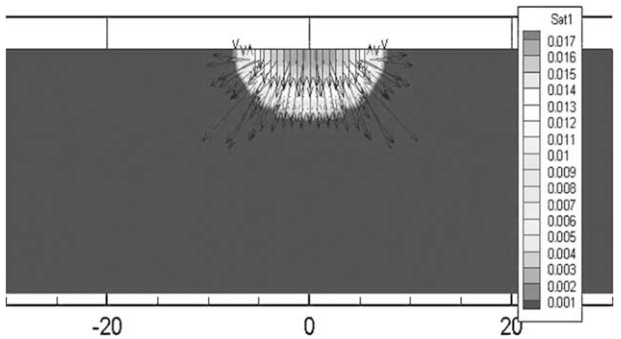

Figure 8. Sulfuric acid within the pores of the sand/sodium sulfide mixture (indicated by saturation = *V*fluid/*V*void, here at *t* = 1.75 h).

The liquid flows (flow direction vectors) out and away from the wetted footprint while reacting with sodium sulfide present in the sand.

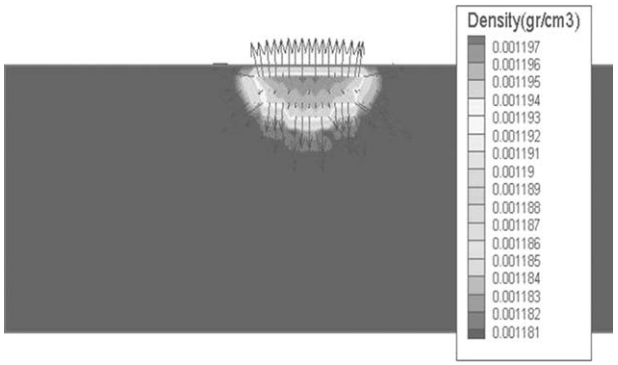

Figure 9. Velocity vectors for hydrogen sulfide gas formed by the reaction of sulfuric acid and sodium sulfide, superimposed on a contour plot of gas density.

Gas flows out of the open upper bound and away from the droplet periphery and then upward.

high concentration to those with lower, such as those located at the periphery of the wetted region. Although the gas-phase solution appears to follow a path that reflects the physics assumed to occur, neither local acid concentrations nor measurement of local gas evolution were made in the experimental study. The data gathered reflected the intent of the experiments: to provide input for the development of a global measurement tool. In the future, experiments designed to evaluate local effects will help further validate the model's algorithms.

Although this study indicates that the chemical reaction algorithm developed within the COMCAD model is capable simulating liquid and solid reactions, there are several limitations to this study. First, while the liquid/solid reaction studied indicated that the evolution of a product gas match expected physics, no gas/gas or gas/solid-phase reaction was modeled. The reaction algorithm in the gas phase mirrors that in the other phases, and therefore it is anticipated to meet similar success. However, additional study is required to evaluate the model's ability to model reactions occurring within the gas phase. These cases were not the focus of this study, but will be explored in future work.

Further model development is required to simulate systems where temperatures vary. In these experiments, the reactions were reasonably characterized as isothermal and the experiments took place at constant temperature. In the environment, the temperature may vary in due to daily temperature cycles and along the time course of chemical degradation. The model is capable of updating reaction rate and material properties, given knowledge of the temperature dependence of the reaction rate. Therefore, this modeling strategy may be employed to model these slowly varying temperatures, using a series of constant temperature steps. However, experimental data to verify this function is not currently available. In the case of an agent deployed via an explosive event, or agent destruction via fire, the model formulation is likely insufficient. These situations while important were not the focus of this development. In addition, reactions that are highly exo/endothermic, cannot be modeled using this model formulation. Inclusion of the energy equation in the model formulation will make these efforts feasible.

Further model development is also required for conditions where adsorption or local micromechanics may strongly influence fluid mixing and reaction. Future model development will include study of these effects.

Conclusions

The COMCAD model is designed to be a general-purpose computational tool for the transport and chemical reaction in porous media. Reactants and products can appear in all phases (solid, liquid, and gas). The governing equations are discretized on a finite difference computational mesh and the droplet topology is described by an overlaid mesh on the top of the domain. The droplet can be place on the lower or upper boundaries. The model demonstrated the ability to predict the total amounts and the distribution of reactants and products present in a porous media as a function of time. The model prediction exhibited the qualitative and quantitative trends observed in the experimental data. These responses indicate a robustness and accuracy in the model.

Acknowledgments

This work was performed with financial supported from the Defense Threat Reduction Agency. The COMCAD model was developed for and is the property of that agency.

Literature Cited

1. Kilpatrick WT, Ling EE, Hin ART, Brevett CAS, Fagan MW, Murdock WP Jr. Experimental design requirements for predictive model development using agent fate wind tunnels. *Air Force Research Laboratory Technical Report*. Report number: AFRL-HE-WP-TR-2004, 2008.
2. Savage JJ. Agent fate program overview. *Scientific Conference on Chemical Biological Defense Research*. MD: Hunt Valley, 2006.
3. Savage JJ. Agent fate program overview. *74th Military Operations Research Society Symposium (MORSS)*. CO: Colorado Springs, 2006.
4. Munro NB, Talmage SS, Griffin GD, Waters LC, Watson AP, King JF. Hauschild V. *Environ Health Perspec*. 1999;107:933.
5. Navaz HK, Chan E, Markivevic B. Convective evaporation model of sessile droplets in a turbulent flow – comparison with wind tunnel data. *Int J Thermal Sci*. 2008;47:953–971.
6. Markicevic B, Li H, Sikorski Y, Zand A, Sanders M, Navaz H. Infiltration time and imprint shape of a sessile droplet imbibing porous media. *J Colloid Interface Sci*. 2009;336:698–706.
7. D'Onofrio T, Navaz H, Markicevic B, Mantooth B, Sumpter K. Experimental and numerical study of spread and sorption of VX sessile drops into medium grain size sand. *Langmuir*. 2010;26:3317–3322.
8. Navaz HK, Zand A, Markicevic B, Herman M, Atkinson T, Li H, Nowakowski A, Gheresus P II, Rothstein M, Kiple J, Middleton V. *Agent Fate Model Integration: Final Report*. Edgewood Chemical and Biological Center (ECBC), Aberdeen Proving Grounds, MD, 2011.
9. Nikolopoulos N, Theodorakakos A, Bergeles G. A numerical investigation of the evaporation process of a liquid droplet impinging onto a hot substrate. *Int J Heat Mass Transfer*. 2007;50:303–319.
10. Zadražil A, Stepanek F, Matar OK. Droplet spreading, imbibition and solidification on porous media. *J Fluid Mech*. 2006;562:1–33.
11. Reis NC Jr, Griffiths RF, Mantle MD, Gladden LF. Investigation of the evaporation of embedded liquid droplets from porous surfaces using magnetic resonance imaging. *Int J Heat Mass Transfer*. 2003;46(7):1279–1292.
12. Brevett CAS, Sumpter K, Pence J, Nickol R, King B, Giannaras C, Durst HD. Evaporation and degradation of VX on silica sand. *J Phys Chem*. 2009;113(16):6622–6633.
13. Brevett CAS, Sumpter K, Wagner GW, Rice JS. Degradation of the blister agent sulfur mustard, bis(2-chloroethyl) sulfide, on concrete. *J Hazard Mater*. 2007;140:353–360.
14. Wagner GW, O'Connor RJ, Edwards JL, Brevett CAS. Effect of drop size on the degradation of VX in concrete. *Langmuir*. 2004;20:7146–7150.

15. Bear J. *Dynamics of Fluids in Porous Media*. New York: Dover Publications, 1988.
16. Vafai K. *Handbook of Porous Media*. New York: Marcel Dekker, 2000.
17. Bear J, Corapcioglu MY, editors. Numerical modeling of multiphase flow in porous media. *Proceedings of NATO Advanced Study Institute on Fundamentals of Transport Phenomena in Porous Media*. Newark, Delaware: Martinus Nijhoff publishers; July 14–23, 1985, 71 p.
18. Chen Q, Balcom BJ. Measurement of rock core capillary pressure curves using a single-speed centrifuge and one dimensional magnetic resonance imaging. *J Chem Phys* 2005;122:214720.
19. Brooks RH, Corey AT. *Hydraulic Properties of Porous Media*. Hydrology Paper No. 3. Fort Collins, CO: Colorada State University, 1964:1.
20. van Genuchten MT. A Closed-form equation for predicting the hydraulic conductivity of unsaturated Soils. *Soil Sci Soc Am J*. 1980; 44:892.
21. Leverett MC. Papers—engineering research—capillary behavior in porous solids (T.P. *1223, with discussion). AIME Trans*. 1941;142:152.
22. Udell KS. Heat transfer in porous media considering phase change and capillarity—the heat pipe effect. *Int J Heat Mass Transfer*. 1985;28:485–495.
23. Navaz HK, Markicevic B, Zand AR, Sikorski Y, Chan E, D'Onofrio TG. Sessile droplet spread into porous substrates - determination of capillary pressure using a continuum approach. *J Colloid Interface Sci*. 2008;325:440–446.
24. Zarrouk SJ. Simulation of complex multi-phase, multi-component reacting flows in porous media. PhD thesis, The University of Auckland, Auckland, New Zealand, 2004.
25. Zarrouk SJ. Reacting Flows in Porous Media: Complex Multi-Phase, Multi-Component Simulation. Saarbrucken, Germany: VDM Verlag Dr. Muller, 2008.
26. Xu T, Sonnenthal EL, Spycher N, Pruess K. *TOUGHREACT User's Guide: A Simulation Program for Non-Isothermal Multiphase Reactive Geochemical Transport in Variably Saturated Geologic Media*. Report LBNL-55460. Berkeley, California: Lawrence Berkeley National Laboratory, 2004.
27. Lichtner PC. Contiuum model for simultaneous chemical reactions and mass transport in hydrothermal systems. *Geochem Cosmochem Acta*. 1985;49:779–800.
28. Steefel CI. *GIMRT, Version 1.2: Software for Modeling Multicomponent, Multidimensional Reactive Transport, User's Guide*. Report UCRL-MA-143182, Livermore, California: Lawrence Livermore National Laboratory, 2001.
29. Treyball RE., *Mass-Transfer Operation*. New York: McGraw Hill, 1980.
30. Navaz HK, Zand A, Atkinson T, Nowakowski A, Kiple J, Kamensky K, Jovic Z. *Agent Fate Modeling-COMCAD Theory and Analysis, Code Structure, and Users Guide (Volume I, II, and III)*. Edgewood Chemical and Biological Center (ECBC), Aberdeen Proving Ground, MD, January 7, 2013.
31. GRIDGEN. *Pointwise Corporation*, Texas: Fort Worth, 2012
32. Wolfe NL, Zepp RG, Gordon JA, Baughman GL, Cline DM. Kinetics of chemical degradation of malathion in water. *Environ Sci Technol*. 1977;11(1):88–93.
33. Markicevic B, D'Onofrio TG, Navaz HK. On spread extent of sessile droplet into porous medium: numerical solution and comparisons with experiments. *Phys Fluids*. 2010;22:012103.
34. Centeno G, Sanchez-Reyna G, Ancheyta J, Munoz JAD, Cardona N. Testing various mixing rules for calculation of viscosity of petroleum blends. *Fuel*. 2011;90(12):3561–3570.

Manuscript received July 23, 2013, and revision received Feb. 10, 2014.